

DETECTING CANDIDATE COSMIC BUBBLE COLLISIONS WITH OPTIMAL FILTERS

J. D. MCEWEN¹, S. M. FEENEY¹, M. C. JOHNSON², H. V. PEIRIS¹

¹*Department of Physics and Astronomy, University College London, London WC1E 6BT, U.K.*

²*Perimeter Institute for Theoretical Physics, Waterloo, Ontario N2L 2Y5, Canada*

Abstract

We review an optimal-filter-based algorithm for detecting candidate sources of unknown and differing size embedded in a stochastic background, and its application to detecting candidate cosmic bubble collision signatures in Wilkinson Microwave Anisotropy Probe (WMAP) 7-year observations. The algorithm provides an enhancement in sensitivity over previous methods by a factor of approximately two. Moreover, it is optimal in the sense that no other filter-based approach can provide a superior enhancement of these signatures. Applying this algorithm to WMAP 7-year observations, eight new candidate bubble collision signatures are detected for follow-up analysis.

1 Introduction

The standard Λ CDM concordance cosmological model is now well supported by observational evidence. However, there are many theoretically well-motivated extensions of Λ CDM that predict detectable secondary signals in the cosmic microwave background (CMB) that are subdominant and consistent with current observational constraints. One such example is the signature of cosmic bubble collisions which arise in models of eternal inflation¹. The most unambiguous way to test cosmic bubble collision scenarios is to determine the full posterior probability distribution of the global parameters defining the theory. However, the enormous size of modern CMB datasets, such as Wilkinson Microwave Anisotropy Probe² (WMAP) and Planck³ observations, make a full-sky evaluation of the posterior at full resolution computationally impractical. Recently, however, a method for approximating the full posterior has been developed^{4,5}. This approach requires preprocessing of the data to recover a set of candidate sources which are most likely to give the largest contribution to the marginalized likelihood used in the calculation of the posterior. The preprocessing stage of this method is thus crucial to its overall effectiveness. Candidate source detection aims to minimise the number of false detections while remaining sensitive to a weak signal; a manageable number of false detections is thus tolerated, as false detections will not significantly contribute to the marginalized likelihood. In these proceedings we review the recent work by McEwen *et al.* (2012)⁶, where we developed an optimal-filter-based candidate source detection algorithm that we applied to detect candidate bubble collision signatures in WMAP data.

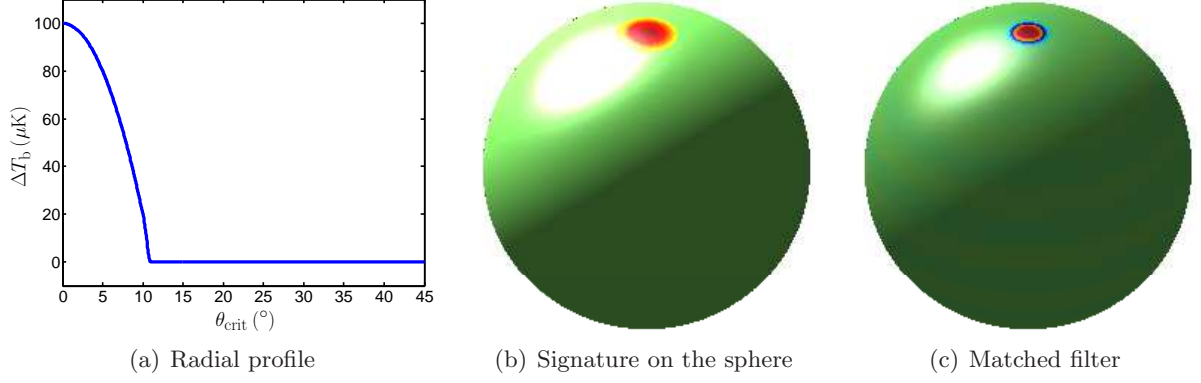


Figure 1: Panels (a) and (b) show the radial profile and spherical plot, respectively, of a bubble collision signature with parameters $\{z_0, \theta_{\text{crit}}, \theta_0, \varphi_0\} = \{100 \mu\text{K}, 10^\circ, 0^\circ, 0^\circ\}$. In panel (c) the corresponding matched filter is shown for the case where the background noise is specified by the CMB.

2 Optimal detection of candidate bubble collisions

Bubble collisions induce a modulative and additive contribution to the temperature fluctuations of the CMB^{4,7}, however the modulative component is second order and may be safely ignored. The additive contribution induced in the CMB by a bubble collision is given by the azimuthally-symmetric profile

$$\Delta T_b(\theta, \varphi) = [c_0 + c_1 \cos(\theta)] s(\theta; \theta_{\text{crit}}), \quad (1)$$

when centered on the North pole, where $(\theta, \varphi) \in S^2$ denote the spherical coordinates of the unit sphere S^2 , with colatitude $\theta \in [0, \pi]$ and longitude $\varphi \in [0, 2\pi)$, c_0 and c_1 are free parameters, $s(\theta; \theta_{\text{crit}})$ denotes a “Schwartz” step function (an infinitely continuous step function that approximates the Heaviside step function) and θ_{crit} is the size of the bubble collision signature. Bubble collision signatures may occur at any position on the sky (θ_0, φ_0) and at a range of sizes θ_{crit} and amplitudes $z_0 = c_0 + c_1$ (we restrict our attention to bubble signatures with zero amplitude at their causal boundaries due to theoretical motivations^{8,9}, *i.e.* $z_{\text{crit}} = c_0 + c_1 \cos(\theta_{\text{crit}}) \sim 0 \mu\text{K}$). A typical bubble collision signature is illustrated in Fig. 1.

We first construct matched filters to detect candidate bubble collision signatures for a known source size, before describing an algorithm for detecting multiple candidate bubble collision signatures of unknown and differing sizes. Matched filters are constructed on the sphere for a given candidate signature size θ_{crit} following the methodology derived by Schaefer *et al.* (2006)¹⁰ and McEwen *et al.* (2008)¹¹. The matched filter corresponding to a typical bubble signature embedded in the CMB is shown in Fig. 1. We construct and apply matched filters for a grid of scales θ_{crit} and then construct significance maps from each filtered field using simulated noise realisations. Potential candidate sources are recovered from the local peaks of thresholded significance maps. We then look across scales and eliminate potential detections if a stronger potential detection is made on an adjacent scale. In this manner we are able to detect candidate bubble collision signatures of unknown and differing size. Further details on the algorithm are given by McEwen *et al.* (2012)⁶, where the approach is shown to perform well on simulations.

3 Bubble collision candidates in WMAP 7-year observations

The algorithm described previously to detect candidate bubble collision signatures was applied⁶ to foreground-cleaned WMAP 7-year W-band observations, once it was calibrated to realistic WMAP observations. The analysis was calibrated using 3,000 Gaussian CMB WMAP simulations with W-band beam and anisotropic instrumental noise to compute the background mean

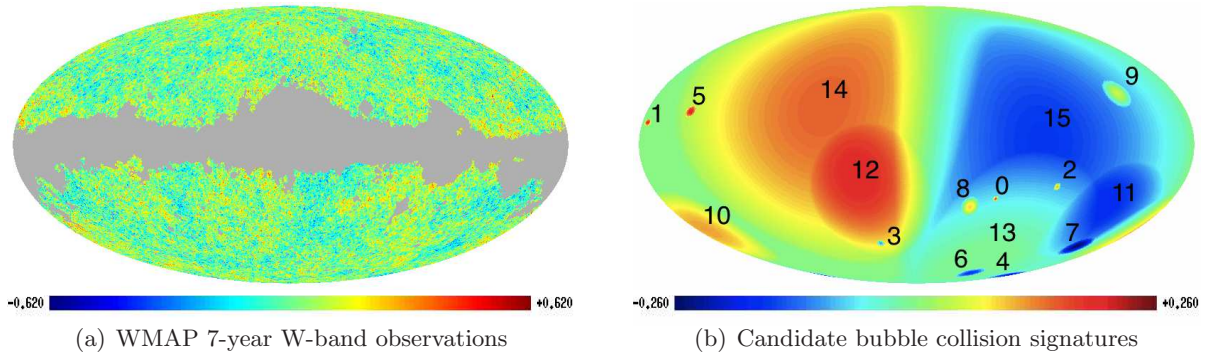


Figure 2: WMAP data analysed by the bubble collision detection algorithm are shown in panel (a) and the resulting candidate bubble collision signatures detected are shown in panel (b) (in units of mK).

and variance required to compute significance maps, for each filter scale. The threshold levels for each scale were calibrated from a realistic WMAP simulation that did not contain bubble collision signatures. The thresholds were chosen to allow a manageable number of false detections while remaining sensitive to weak bubble collision signatures. For this calibration a complete end-to-end simulation of the WMAP experiment provided by the WMAP Science Team¹² was used. Throughout the calibration the WMAP KQ75 mask¹² was adopted.

The calibrated bubble collision detection algorithm was applied⁶ to foreground-cleaned WMAP 7-year W-band observations¹³, with the conservative KQ75 mask¹² applied. The WMAP W-band data that were analysed and the detected candidates are plotted on the full-sky in Fig. 2. Sixteen candidate bubble collision signatures were detected, including eight new candidates that have not been reported by previous studies. The parameters of the detected candidate signatures are reported by McEwen *et al.* (2012)⁶.

4 Conclusions

We have reviewed the work by McEwen *et al.* (2012)⁶, where an algorithm for detecting candidate cosmic bubble collision signatures in CMB observations was developed and applied. The algorithm is based on the application of optimal filters on the sphere and thus it is optimal in the sense that no other filter-based approach can provide a superior enhancement of bubble collision signatures. Furthermore, the approach is general and applicable to the detection of other sources on the sphere embedded in a stochastic background. After calibrating the algorithm on realistic WMAP simulations, it was applied to WMAP 7-year observations. Sixteen candidate bubble collision signatures were detected, including eight new candidates that have not been reported by previous studies. To ascertain whether these detections are indeed bubble collision signatures or merely rare Λ CDM fluctuations, it is necessary to use the candidates detected by the optimal-filter-based algorithm to construct the full posterior^{4,5} and perform a robust model selection analysis; this is the focus on ongoing work.

Acknowledgments

We thank Daniel Mortlock for useful discussions. SMF thanks David Spergel for an interesting related conversation. We are very grateful to Eiichiro Komatsu and the WMAP Science Team for supplying the end-to-end WMAP simulations used in our null tests. This work was partially supported by a grant from the Foundational Questions Institute (FQXi) Fund, a donor-advised fund of the Silicon Valley Community Foundation on the basis of proposal FQXi-RFP3-1015 to the Foundational Questions Institute. JDM was supported by a Leverhulme Early Career Fel-

lowship from the Leverhulme Trust throughout the completion of this work and is now supported by a Newton International Fellowship from the Royal Society and the British Academy. SMF is supported by the Perren Fund and STFC. Research at Perimeter Institute is supported by the Government of Canada through Industry Canada and by the Province of Ontario through the Ministry of Research and Innovation. HVP is supported by STFC and the Leverhulme Trust. We acknowledge use of the HEALPix package and the Legacy Archive for Microwave Background Data Analysis (LAMBDA). Support for LAMBDA is provided by the NASA Office of Space Science.

References

1. Anthony Aguirre, Matthew C Johnson, and Assaf Shomer. Towards observable signatures of other bubble universes. *Phys. Rev. D.*, D76:063509, 2007.
2. C. L. Bennett, M. Bay, M. Halpern, G. Hinshaw, C. Jackson, N. Jarosik, A. Kogut, M. Limon, S. S. Meyer, L. Page, D. N. Spergel, G. S. Tucker, D. T. Wilkinson, E. Wollack, and E. L. Wright. The Microwave Anisotropy Probe Mission. *Astrophys. J.*, 583:1–23, January 2003.
3. J. A. Tauber, N. Mandolesi, J.-L. Puget, et al. Planck pre-launch status: The Planck mission. *Astron. & Astrophys.*, 520, September 2010.
4. Stephen M. Feeney, Matthew C. Johnson, Daniel J. Mortlock, and Hiranya V. Peiris. First observational tests of eternal inflation: Analysis methods and wmap 7-year results. *Phys. Rev. D.*, D84:043507, 2011.
5. Stephen M. Feeney, Matthew C. Johnson, Daniel J. Mortlock, and Hiranya V. Peiris. First observational tests of eternal inflation. *Phys. Rev. Lett.*, 107:071301, 2011.
6. J. D. McEwen, S. M. Feeney, M. C. Johnson, and H. V. Peiris. Optimal filters for detecting cosmic bubble collisions. *Phys. Rev. D.*, in press, 2012.
7. Spencer Chang, Matthew Kleban, and Thomas S. Levi. Watching Worlds Collide: Effects on the CMB from Cosmological Bubble Collisions. *JCAP*, 0904:025, 2009.
8. Roberto Gobetti and Matthew Kleban. Analyzing Cosmic Bubble Collisions. 2012.
9. Matthew Kleban, Thomas S. Levi, and Kris Sigurdson. Observing the Multiverse with Cosmic Wakes. 2011.
10. Bjoern Malte Schaefer, Christoph Pfrommer, Reinhard M. Hell, and Matthias Bartelmann. Detecting Sunyaev-Zel’dovich clusters with Planck: II. Foreground components and optimised filtering schemes. *Mon. Not. Roy. Astron. Soc.*, 370:1713–1736, August 2006.
11. J. D. McEwen, M. P. Hobson, and A. N. Lasenby. Optimal filters on the sphere. *IEEE Trans. Sig. Proc.*, 56(8):3813–3823, 2008.
12. B. Gold, N. Odegard, J. L. Weiland, R. S. Hill, A. Kogut, C. L. Bennett, G. Hinshaw, X. Chen, J. Dunkley, M. Halpern, N. Jarosik, E. Komatsu, D. Larson, M. Limon, S. S. Meyer, M. R. Nolte, L. Page, K. M. Smith, D. N. Spergel, G. S. Tucker, E. Wollack, and E. L. Wright. Seven-year Wilkinson Microwave Anisotropy Probe (WMAP) Observations: Galactic Foreground Emission. *Astrophys. J. Supp.*, 192:15, February 2011.
13. N. Jarosik, C. L. Bennett, J. Dunkley, B. Gold, M. R. Greason, M. Halpern, R. S. Hill, G. Hinshaw, A. Kogut, E. Komatsu, D. Larson, M. Limon, S. S. Meyer, M. R. Nolte, N. Odegard, L. Page, K. M. Smith, D. N. Spergel, G. S. Tucker, J. L. Weiland, E. Wollack, and E. L. Wright. Seven-year Wilkinson Microwave Anisotropy Probe (WMAP) Observations: Sky Maps, Systematic Errors, and Basic Results. *Astrophys. J. Supp.*, 192:14, February 2011.